

# Pion and Proton Form Factors in the Regge Description of Electroproduction $p(e, e'\pi^+)n$

Tae Keun CHOI\*

*Department of Physics, Yonsei University, Wonju 26493, Korea*

Kook Jin KONG† and Byung Geel YU‡

*Research Institute of Basic Sciences, Korea Aerospace University, Goyang 10540, Korea*

(Received 4 August 2015, in final form 17 August 2015)

Electroproduction of  $\pi^+$  above the resonance region is analyzed in the Regge model for  $\pi + \rho$  exchanges. The importance of the roles of the pion and the proton form factors in the process is discussed in comparison with the existing models of Kaskulov and Mosel and of Vrancx and Ryckebusch. The present model with a proton form factor of a simple dipole-type is shown to yield a better description of DESY and JLab data over those models for the high  $Q^2$  and  $-t$  region up to 5 GeV<sup>2</sup>.

PACS numbers: 21.10.Ft, 24.10.-i

Keywords: Pion, Electroproduction, Regge pole model, Regge phenomenology, Dirac form factor, Proton form factor, Pion form factor, Dipole form factor

DOI: 10.3938/jkps.67.1089

Recent experiments on the electroproduction of  $\pi^+$  at JLab has drawn attention because the data from the experiment cover a wide range of the photon momentum transfer  $Q^2$  at high energy  $W$  [1–3]. Analyses of electroproduction data have shown that the cross sections of the process are largely determined by the pion and the nucleon electromagnetic form factors that include information about the hadron structure [4–6]. Therefore, electroproduction plays a role not only in understanding the production mechanism but also in testing various sorts of form factors originating either from phenomenological or from some theoretical basis on Quantum Chromodynamics (QCD) [5,7].

One interesting feature of the process is that empirical data at large momentum transfer  $Q^2$  and high energy  $W$  require a large contribution of the  $s$ -channel proton pole to the transverse cross section  $d\sigma_T/dt$  in order to reproduce a set of four separated differential cross sections,

$$2\pi \frac{d\sigma}{dt d\phi} = \frac{d\sigma_T}{dt} + \epsilon \frac{d\sigma_L}{dt} + \epsilon \frac{d\sigma_{TT}}{dt} \cos 2\phi + \sqrt{2\epsilon(\epsilon+1)} \frac{d\sigma_{LT}}{dt} \cos \phi, \quad (1)$$

in a consistent manner. The longitudinal cross section  $d\sigma_L/dt$  follows the pion-pole dominance with the form

factor  $F_\pi(Q^2)$  of a monopole type from  $\rho$ -meson dominance, as expected from

$$d\sigma_L \propto |g_{\pi NN} F_\pi(Q^2)|^2. \quad (2)$$

For an enhancement of  $s$ -channel exchange, therefore, in the Regge model for  $t$ -channel meson exchange, Kaskulov and Mosel (KM) [5] introduced an  $s$ -dependence of the charge form factor  $F_s$  to the proton pole term to implement the contributions of the  $N^*$  resonances based on the Bloom-Gilman duality [8], *i.e.*,

$$F_s(Q^2, s) = \frac{\int_{M_p^2}^{\infty} ds_i \frac{s_i^{-\beta}}{s-s_i+i0^+} \left(1 + \xi \frac{Q^2}{s_i}\right)^{-2}}{\int_{M_p^2}^{\infty} ds_i \frac{s_i^{-\beta}}{s-s_i+i0^+}}, \quad (3)$$

which results in Eq. (43) of Ref. 5. Within a framework similar to that of KM, Vrancx and Ryckebusch (VR) showed a fit of cross sections by using the proton charge form factor  $F_s$  of a dipole type [6],

$$F_p(Q^2, s) = (1 + Q^2/\Lambda_{\gamma pp}^2(s))^{-2}, \quad (4)$$

in which case the cutoff mass has an energy  $s$ -dependence. As shown in Ref. [6], however, the validity of such form factors of proton in these works are questionable for the large  $-t$  region, which is particularly true for very recent data [3].

In this work we investigate the process

$$\gamma^*(k) + p(p) \rightarrow \pi^+(q) + n(p') \quad (5)$$

\*E-mail: tkchoi@yonsei.ac.kr

†E-mail: kong@kau.ac.kr

‡E-mail: bgyu@kau.ac.kr

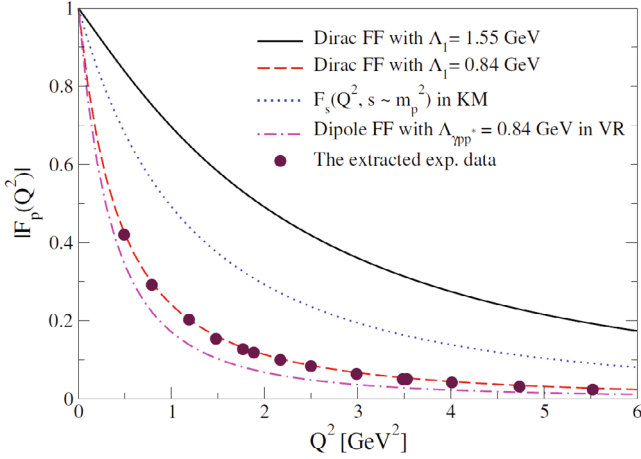


Fig. 1. (Color online) The  $Q^2$ -dependence of proton charge form factors used in the models of Refs. [5] and [6] and the present work. The curves from KM and VR are estimated at  $s = M_p^2$ .

based on an extension of our previous works [9] to electroproduction. Our purpose here is to find another set of possible parameters for the pion and the proton charge form factors to fit the cross sections. Avoiding complications in the parameterization of the proton charge form factor as in Eqs. (3) and (4), we reconsider the proton form factor of a simple dipole type as in Eq. (4), but now it has a constant cutoff mass that can be adjusted. We then examine whether that proton form factor is valid up to  $-t \approx 5 \text{ GeV}^2$  at large  $Q^2$  and high energy  $W$ .

For clarity, we work with a simple model consisting of  $\pi + \rho$  Regge pole exchanges. In order to maintain gauge invariance of the production amplitude, we have used the Gross-Riska prescription [10] for proton and pion charge form factors to constrain the respective longitudinal components from coupling to virtual photon. Thus, the production amplitude can be written as

$$\mathcal{M} = \bar{u}_N(p')\sqrt{2}[\mathcal{M}_{s,p} + \mathcal{M}_{t,\pi} + \mathcal{M}_{t,\rho}]u_N(p), \quad (6)$$

with

$$i\mathcal{M}_{s,p} = eg_{\pi NN}\gamma_5 \frac{(\not{p} + \not{k} + M_p)}{s - M_p^2} \tilde{F}_1(Q^2)\not{\epsilon}, \quad (7)$$

$$i\mathcal{M}_{t,\pi} = eg_{\pi NN}\tilde{F}_\pi(Q^2) \frac{(2q - k) \cdot \epsilon}{t - m_\pi^2} \gamma_5, \quad (8)$$

$$i\mathcal{M}_{t,\rho} = -ig_{\gamma\rho\pi}g_{\rho NN}F_\rho(Q^2)\epsilon^{\mu\nu\alpha\beta}\epsilon_\mu k_\nu q'_\alpha \times \left( \gamma_\beta + \frac{\kappa_\rho}{4m_p}[\gamma_\beta, \not{q}'] \right), \quad (9)$$

where  $\tilde{F}_1(Q^2)\not{\epsilon}$  and  $\tilde{F}_\pi(Q^2)(2q - k)^\mu$  are

$$(F_1(k^2) - F_1(0)) \left( \not{\epsilon} - \not{k} \frac{k \cdot \epsilon}{k^2} \right) + F_1(0)\not{\epsilon}, \quad (10)$$

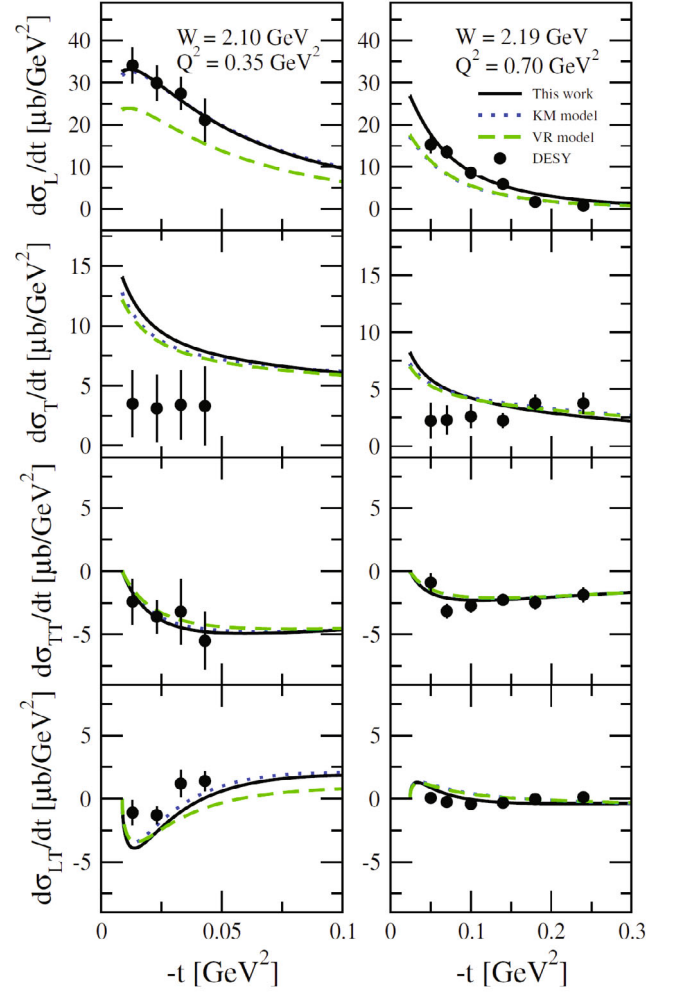


Fig. 2. (Color online) Differential cross sections at very forward angles  $-t < 0.3 \text{ GeV}^2$  and small  $Q^2$ . The solid line results from the present work with  $\Lambda_\pi = 0.78 \text{ GeV}$  and  $\Lambda_1 = 1.55 \text{ GeV}$ . The dotted line is from the KM model with  $\Lambda_\pi = 0.775$  (left) and  $0.63$  (right)  $\text{GeV}$  and  $F_s(Q^2, s)$  in Eq. (43) in Ref. 5. The dashed line is from the VR model with  $\Lambda_\pi = 0.655 \text{ GeV}$  and  $F_p(Q^2, s)$  in Eq. (4). Data are taken from Ref. [14] for  $Q^2 = 0.35 \text{ GeV}^2$  and from Ref. [15] for  $Q^2 = 0.7 \text{ GeV}^2$  (DESY).

$$(F_\pi(k^2) - F_\pi(0))(2q - k) \cdot \left( \epsilon - k \frac{k \cdot \epsilon}{k^2} \right) + F_\pi(0)(2q - k) \cdot \epsilon, \quad (11)$$

respectively.  $Q^2 = -k^2$  is the virtual photon momentum and  $q' = q - k$  is the  $t$ -channel momentum transfer. The gauge-invariant  $\rho$  meson exchange is denoted by  $\mathcal{M}_{t,\rho}$ , with the transition form factor  $F_\rho(Q^2)$  at the  $\gamma\rho\pi$  coupling vertex with the coupling constant  $g_{\gamma\rho\pi} = 0.22 \text{ GeV}^{-1}$ . For the meson-baryon coupling constants, we use  $g_{\pi NN} = 13.4$  and  $g_{\rho NN} = 3.4$  with  $\kappa_\rho = 6.1$ .

To reggeize the  $t$ -channel meson exchange, we simply replace the Feynmann pole with the Regge pole which

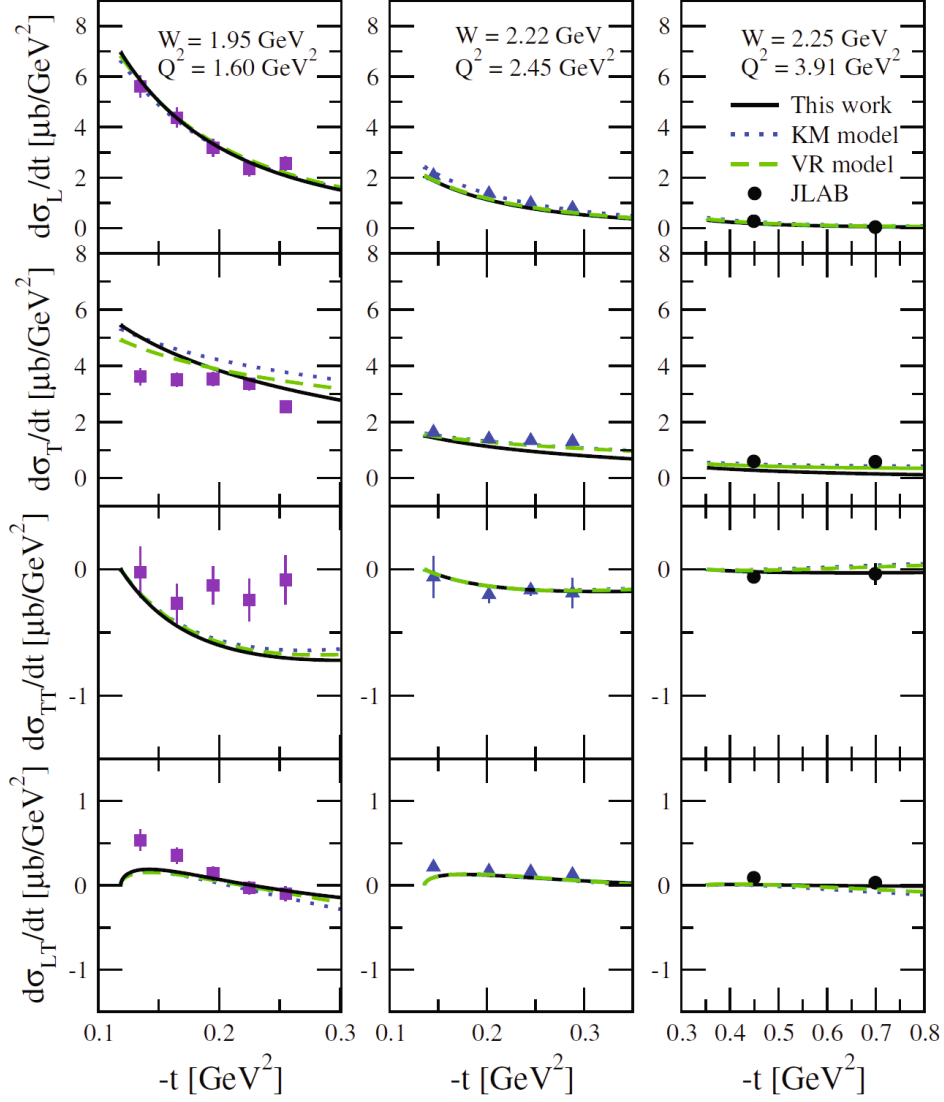


Fig. 3. (Color online) Differential cross sections at forward angles  $-t < 1$  and  $Q^2$  up to  $4 \text{ GeV}^2$ . The solid line results from the present work with  $\Lambda_\pi = 0.65 \text{ GeV}$  and  $\Lambda = 1.55 \text{ GeV}$ . Notations are the same as in Fig. 2 for the dotted line with  $\Lambda_\pi = 0.68 \text{ GeV}$  and the dashed line with  $\Lambda_\pi = 0.655 \text{ GeV}$ . Data are taken from the F $\pi$ -1 [16] (squares), F $\pi$ -2 [1,17] (triangles), and  $\pi$ -CT [2] (circles) experiments at JLab.

can be collectively written as

$$\mathcal{R}^\varphi(s, t) = \frac{\pi \alpha'_\varphi}{\Gamma(\alpha_\varphi(t) + 1 - J)} \frac{\frac{1}{2}((-1)^J + e^{-i\pi\alpha_\varphi})}{\sin \pi\alpha_\varphi(t)} \left(\frac{s}{s_0}\right)^{\alpha_\varphi(t) - J} \quad (12)$$

for the  $\varphi$  meson of arbitrary spin  $J$ . In the present work, we use the complex phase  $e^{-i\pi\alpha(t)}$  for both the  $\pi$  and the  $\rho$  exchanges with the trajectories

$$\alpha_\pi(t) = 0.7(t - m_\pi^2), \quad (13)$$

$$\alpha_\rho(t) = 0.83t + 0.53, \quad (14)$$

respectively.

Let us now discuss how to choose the pion and the proton charge form factors in Eqs. (10) and (11), which

are needed to model the  $\pi^+$  electroproduction process. In the small  $-t$  and low  $Q^2$  region (see Fig. 2 below, for instance), cross section data show the longitudinal cross section  $d\sigma_L/dt$  to be large in comparison to the others. This is a manifestation of the dominance of the pion exchange with the charge form factor

$$F_\pi(Q^2) = \frac{1}{1 + Q^2/\Lambda_\pi^2}, \quad (15)$$

which is parameterized as a monopole-type from the vector meson dominance. The cutoff mass is, therefore,  $\Lambda_\pi = m_\rho$ , which is somewhat larger than  $\Lambda_\pi = 0.71 \text{ GeV}$  fitted to the measurement of the on-shell form factor in the elastic  $eN$  scattering process. In the  $\gamma^*p \rightarrow \pi^+n$  process, however, the pion exchange proceeds via off-shell

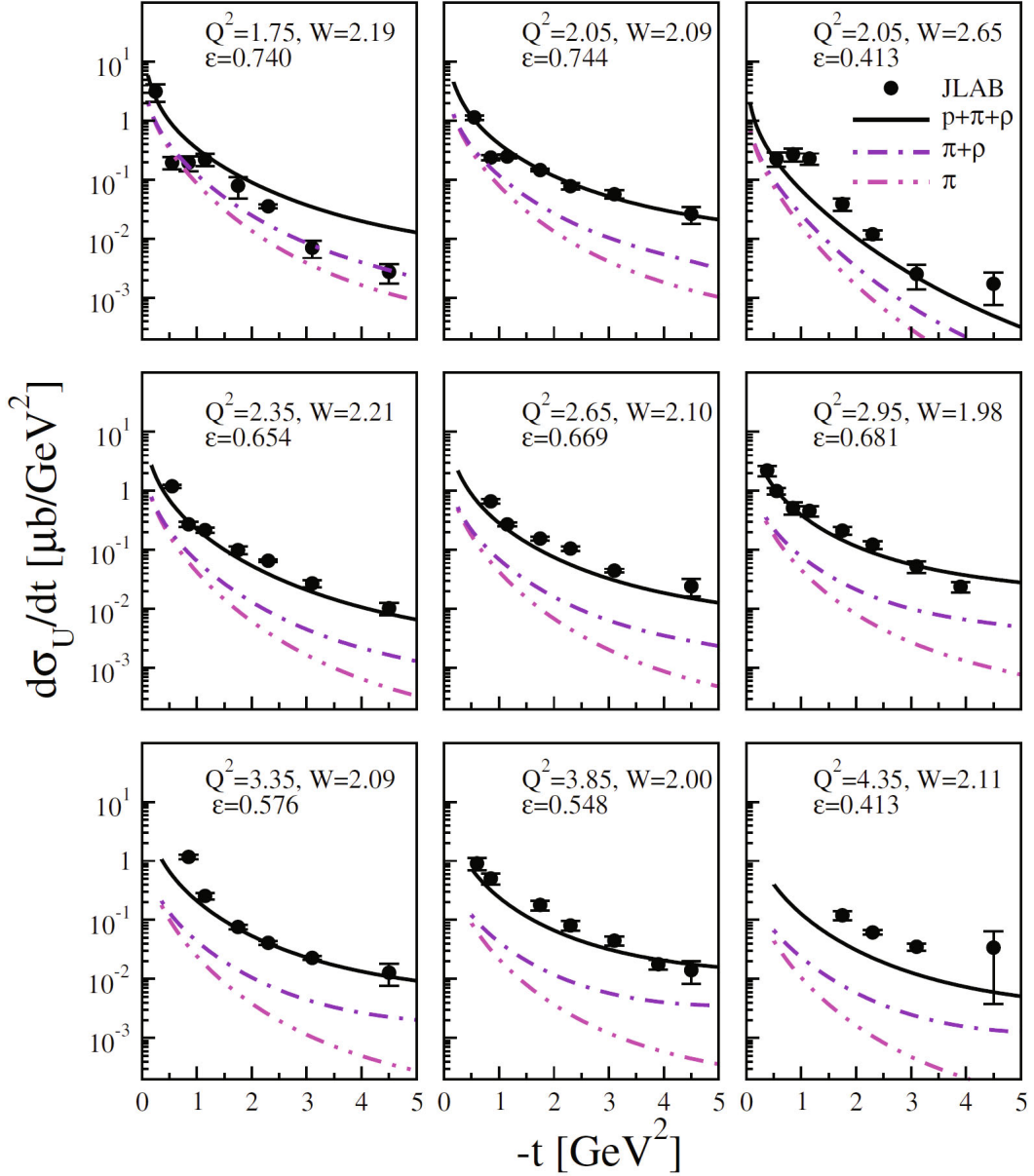


Fig. 4. (Color online) Contribution of the meson exchange in the unseparated cross section  $d\sigma_U/dt$ . The dash-dot-dotted line is the contribution from  $\pi$  exchange. The dash-dotted line corresponds to the contribution of  $\pi + \rho$ . The solid line results from  $p(\text{proton}) + \pi + \rho$  exchanges with  $\Lambda_\pi = 0.65$  GeV and  $\Lambda_1 = 1.55$  GeV. Data are taken from Ref. [3].

propagation; we, thus, consider  $\Lambda_\pi$  to be a fitting parameter to be varied in the range  $0.6 \sim 0.8$  GeV in this work.

The proton exchange in the  $s$ -channel, though added to restore gauge invariance, plays a role in the transverse cross section  $d\sigma_T/dt$ , which corresponds to photoproduction of  $\pi^+$  at the photon point  $Q^2 = 0$ . It is reasonable to assume  $N^*$  contributions in the resonance region [5,6]. The  $Q^2$  dependence of the proton form factor, called the Dirac form factor,  $F_1(Q^2)$  is determined from the Sachs electric and magnetic form factors  $G_E(Q^2)$  and  $G_M(Q^2)$

by using the relation

$$F_1(Q^2) = \frac{G_E(Q^2) + \tau G_M(Q^2)}{1 + \tau}, \quad (16)$$

where  $\tau(Q^2) = Q^2/4M_P^2$  and  $F_1(0) = 1$ . In the measurement of the on-shell form factors of a nucleon,  $G_E(Q^2)$  and  $G_M(Q^2)$  are applied and parameterized as

$$G_E(Q^2) = G_D(Q^2), \quad G_M(Q^2) = \mu_p G_D(Q^2), \quad (17)$$

where

$$G_D(Q^2) = (1 + Q^2/\Lambda_1^2)^{-2} \quad (18)$$

of the dipole type with  $\Lambda_1^2 = 0.71 \text{ GeV}^2$  fitted to the empirical data [11].  $G_E(0) = 1$  and  $G_M(0) = \mu_p = 2.793$  normalized for the proton state. As mentioned in the beginning, we adopt in this work the proton charge form factor  $F_1(Q^2)$  given in Eq. (16), together with Eqs. (17), and (18) above. Note that by the definition in Eq. (16), followed by Eqs. (17) and (18), the proton charge form factor  $F_1(Q^2)$  in this work differs not only by the cutoff mass  $\Lambda_{\gamma pp^*}(s)$  but also by the overall factor  $\left(\frac{1+\tau\mu}{1+\tau}\right)$  from that of VR [6] given in Eq. (4).

In Fig. 1, we present the  $Q^2$ -dependence of the proton charge form factors  $F_1(Q^2)$  adopted in the models of KM, VR, and the present work for comparison. The dashed line describes the form factor  $F_1(Q^2)$  in Eq. (18) with  $\Lambda_1 = 0.84 \text{ GeV}$ , which is in good agreement with experimental data of Refs. [12] and [13]. The dotted line is from the transition form factor  $F_s(Q^2, s \rightarrow M_p^2)$  in the KM model (Eq. (43) of Ref. [5]) while the dash-dotted line is from the form factor in Eq. (4) for the VR model. The solid line results from the Dirac form factor  $F_1(Q^2)$  with  $\Lambda_1 = 1.55 \text{ GeV}$  used in the present work.

While differences in the proton form factor among the models are apparent, the cutoff mass  $\Lambda_\pi$  based on the pion form factor in Eq. (15), common to all models, should be different from one another for an agreement with experiment. The KM model divides the cutoff mass into three parts:  $\Lambda_\pi = 0.775 \text{ GeV}$  for  $Q^2 < 0.4 \text{ GeV}^2$ ,  $0.63 \text{ GeV}$  for  $0.6 < Q^2 < 1.5 \text{ GeV}^2$ , and  $0.68 \text{ GeV}$  for  $Q^2 > 1.5 \text{ GeV}^2$ . The VR model fixed  $\Lambda_\pi = 0.655 \text{ GeV}$ , regardless of the  $Q^2$  range with a smaller coupling constant  $g_{\pi NN} = 13.0$ . We use  $\Lambda_\pi = 0.78 \text{ GeV}$  for the DESY data and  $\Lambda_\pi = 0.65 \text{ GeV}$  for the JLab data with the coupling constants concerning  $\pi$  and  $\rho$  being the same as those of the KM model.

Figure 2 shows four differential cross sections resulting from the KM model, the VR model, and the model used in this work for the small  $-t$  and  $Q^2$  region. Note that these model predictions are made within our simple framework of proton  $+\pi+\rho$  exchanges where neglecting the higher-spin meson exchange employed in the KM and the VR models, which is by two orders of magnitude smaller than  $\pi+\rho$ . Therefore, the differences between the models are basically the differences of the proton form factors together with the cutoff  $\Lambda_\pi$ , as discussed above. In this analysis, we fix the cutoff mass  $\Lambda_1 = 1.55 \text{ GeV}$  over whole range of  $Q^2$  and  $-t$  for the proton form factor in Eq. (16) while the VM model uses  $\Lambda_{\gamma pp^*}(s) = 0.84 + (2.19 - 0.84)(1 - M_p^2/s)(\text{GeV})$ . The KM form factor would yield  $\Lambda_1 \approx 1.48 \text{ GeV}$  in the limit of  $s \rightarrow M_p^2$ , as estimated in correspondence with the same form factor for the VM model [6]. Thus, all the cutoff masses for the proton form factors in these models are almost two times larger than the  $\Lambda_1 = 0.84 \text{ GeV}$  fitted to the on-shell form factor from experimental data, suggestive of an  $N^*$  contribution or an off-shell effect in the  $s$ -channel.

In the high- $Q^2$  region, the JLab data for small  $-t$

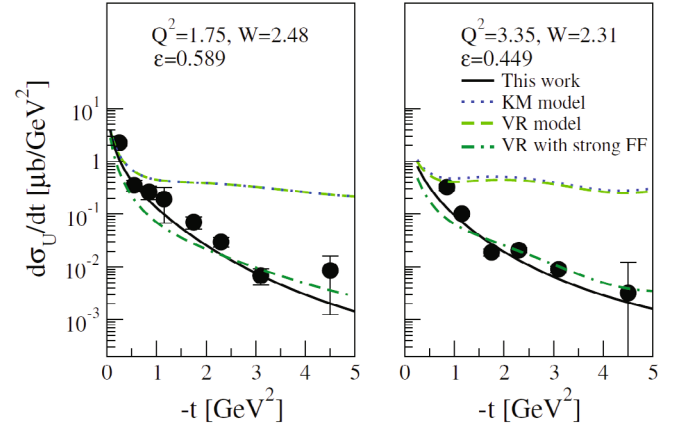


Fig. 5. (Color online)  $-t$  dependence of the unseparated cross section  $d\sigma_U/dt$ . Notations are the same as in Fig. 3 for solid, dotted and dashed lines. The dash-dash-dotted line is from the VR model with the inclusion of the strong hadronic form factor given in Eq. (28) of Ref. 6. Data are taken from Ref. 3.

and large  $-t$  are presented in Fig. 3 and Fig. 4. Our model reproduces those cross sections with a reduced value  $\Lambda_\pi = 0.65 \text{ GeV}$  while using an fixed  $\Lambda_p = 1.55 \text{ GeV}$ , which is independent of  $Q^2$  and  $-t$  momentum transfer.

The change in  $\Lambda_\pi$  due to a variation of  $Q^2$  can be understood as a change in the measurement of the charge radius of pion,

$$\langle r_\pi^2 \rangle = -6 \left. \frac{dF_\pi}{dQ^2} \right|_{Q^2=0} = 6/\Lambda_\pi^2, \quad (19)$$

which reads  $\langle r_\pi^2 \rangle = 0.384 \text{ fm}^2$  for  $\Lambda_\pi = 0.78 \text{ GeV}$  and  $\langle r_\pi^2 \rangle = 0.55 \text{ fm}^2$  for  $\Lambda_\pi = 0.65 \text{ GeV}$ . This is sensible because the size of the pion will increase with higher resolution as  $Q^2$  increases.

Based on the present model with cutoff masses consistent with DESY and JLab data, we analyze the unseparated cross section

$$d\sigma_U = d\sigma_T + \epsilon d\sigma_L \quad (20)$$

at the high  $Q^2$  and large  $-t$  region. We note in Fig. 4 that the contribution of  $\rho$  exchange becomes noticeable in this kinematical region. We should point out that the sign of  $\gamma\rho\pi$  coupling is of importance in reproducing the data. A comparison of model predictions is given in Fig. 5 for the cross section at high  $Q^2$  and  $-t$  up to  $5 \text{ GeV}^2$ . The result confirms the present work to be more reliable for wider applications than the others.

## ACKNOWLEDGMENTS

This work was partly supported by grant NRF-2013R1A1A2010504 from the National Research Foundation (NRF) of Korea.

## REFERENCES

- [1] H. P. Blok *et al.*, Phys. Rev. C **78**, 045202 (2008).
- [2] T. Horn *et al.*, Phys. Rev. C **78**, 058201 (2008).
- [3] K. Park *et al.*, Eur. Phys. J. A **49**, 16 (2013).
- [4] M. Guidal, J.-M. Laget and M. Vanderhaeghen, Phys. Rev. C **61**, 025204 (2000).
- [5] M. M. Kaskulov and U. Mosel, Phys. Rev. C **81**, 045202 (2010).
- [6] T. Vranx and J. Ryckebusch, Phys. Rev. C **89**, 025203 (2014).
- [7] M. Gari and W. Krümpelmann, slac-pub-3398 (1984); Phys. Rev. D **45**, 1817.
- [8] E. D. Bloom and F. J. Gilman, Phys. Rev. Lett. **25**, 1140 (1970).
- [9] B. G. Yu, T. K. Choi and W. Kim, Phys. Rev. C **83**, 025208 (2011).
- [10] F. Gross and D. O. Riska, Phys. Rev. C **36**, 1928 (1987).
- [11] L. N. Hand, D. G. Miller and R. Wilson, Rev. Mod. Phys. **35**, 335 (1963).
- [12] C. F. Perdrisat, V. Punjabi and M. Vanderhaeghen, Prog. Part. Nucl. Phys. **59**, 694 (2007).
- [13] J. J. Kelly, Phys. Rev. C **70**, 068202 (2004).
- [14] H. Ackermann, T. Azemoon, W. Gabriel, H. D. Mer-tiens, H. D. Reich and G. Specht, Nucl. Phys. B **137**, 294 (1978).
- [15] P. Brauel, T. Canzler, D. Cords, R. Felst, G. Grindham-mer, M. Helm, W.-D. Kollmann, H. Krehbiel and M. Sch dlich, Z. Phys. C **3**, 101 (1979).
- [16] V. Tadevosyan *et al.*, Phys. Rev. C **75**, 055205 (2007).
- [17] T. Horn *et al.*, Phys. Rev. Lett. **97**, 192001 (2006).